Electronic Supplementary Information (ESI)

Li(110) Lattice Plane Evolution Induced by 3D MXene Skeleton for Stable Lithium Metal Anodes

Yong-Zheng Fang,[a,b] Sainan Liang,[a] Xu Zhang,[a,c] Junwu Sang,[a] Shasha Gao,[a,d] Zhang Zhang,[a,c] Kai Zhu,[b] Dianxue Cao[b,*] and Zhen Zhou[a,c,*]

[a] School of Chemical Engineering, Zhengzhou University, Zhengzhou 450001, China.

[b] Key Laboratory of Superlight Materials and Surface Technology (Ministry of Education), College of Material Science and Chemical Engineering, Harbin Engineering University, Harbin 150001, China.

[c] School of Materials Science and Engineering, Institute of New Energy Material Chemistry, Renewable Energy Conversion and Storage Center (ReCast), Key Laboratory of Advanced Energy Materials Chemistry (Ministry of Education), Nankai University, Tianjin 300350, China.

[d] Key Laboratory of Microelectronics and Energy of Henan Province, College of Physics and Electronic Engineering, Xinyang Normal University, Xinyang 464000, China.

E-mail: caodianxue@hrbeu.edu.cn; zhenzhou@zzu.edu.cn

Experimental Section

Preparation of $Ti_3C_2T_x$ MXene ultrathin nanosheets

Laminated MXene ($Ti_3C_2T_x$) was obtained by etching the MAX phase (Ti_3AlC_2, 400 mesh, purchased from 11 Technology Co., Ltd.) via synthetic HF solution. Concretely, 4 g LiF (Alfa Aesar, 98.5%) was dissolved in 40 mL HCl (9 M) under stir for 30 min. Then, 2 g Ti_3AlC_2 powders were slowly added to the mixture solution and stirred for 30 h at 40 °C. After centrifugation until neutral, the laminated $Ti_3C_2T_x$ nanosheets slurry was collected. Then, the $Ti_3C_2T_x$ slurry was dispersed in 100 mL DI water and under ultrasound for 20 min, and then, the dispersion was centrifuged at 3500 r for 10 min to collect the above turbid liquid. Repeating this process for three times could obtain more few-layer $Ti_3C_2T_x$. Finally, ultrathin $Ti_3C_2T_x$ nanosheets were obtained by sonicating the obtained dispersion for 20 minutes and centrifuging for 30 minutes again.

Treatment of carbon cloth

Carbon cloth (CC) was washed with DI water and ethyl alcohol under ultrasound. Then it was soaked in concentrated nitric acid for 3 h and then washed with DI water to obtain the wettability for MXene dispersion.

Preparation of $Ti_3C_2T_x$-CC and Li-$Ti_3C_2T_x$-CC

$Ti_3C_2T_x$-CC was fabricated by an electrophoretic deposition process under 5 V constant voltage in 4 $mg \cdot mL^{-1}$ ultrathin $Ti_3C_2T_x$ dispersion. The CC was employed as anode and cathode. The deposition time was selected at 30 s based on the previous report.[1] After air drying, Li-$Ti_3C_2T_x$-CC electrodes were fabricated via a melton Li diffusion process

at 350 ℃ in a glove box, during which a roller pressure procedure was adopted to speed up Li diffusion.

Materials Characterization

The crystal patterns of bare Li, Li-CC, and Li-$Ti_3C_2T_x$-CC were checked by X-ray diffractometer (XRD) with the copper Kα radiation (λ=1.5418Å). To prevent oxidation during the test, the Li metal was covered with parafilm in an Ar-filled glove box. The morphologies of the $Ti_3C_2T_x$ nanosheets, $Ti_3C_2T_x$-CC, Li-$Ti_3C_2T_x$-CC, and electrodes under different states were observed by the transmission electron microscope (TEM, JEOL, JEM-2100 model) and the field-emission scanning electron microscope (SEM, JEOL, JSM7500F). The surface states of $Ti_3C_2T_x$ and $Ti_3C_2T_x$-CC were examined by the X-ray photoelectron spectroscopy (XPS) tests (The surface analysis system (Thermofisher Escalab Xi+) using Al Kα radiation (hν=1486.6 eV) from a monochromatic X-ray source, and a 500-μm light spot size was used).

Electrochemical Measurements

The symmetrical cells were assembled with two same Li-$Ti_3C_2T_x$-CC electrodes or bare Li foil as anode and cathode (1.0*1.0 cm^2). The full cells were assembled with Li-$Ti_3C_2T_x$-CC or bare Li as anode and $LiFePO_4$ as cathode (circle with a diameter of 1.0 cm). Celgard (Whatman) was used as the separator. The electrolytes were 1.0 M $LiPF_6$ in EC/DMC/EMC (1:1:1 Vol %). The CR2023-type coin cells were assembled using the above things in the Ar-filled glove box. Constant current charge-discharge and electrochemical impedance spectroscopy (EIS) tests of the cells were measured on the

NEWARE battery tester and Bio-Logic VMP3 electrochemical workstation, respectively.

Computational Details

In this work, all the computations were performed with the Vienna ab initio Simulation Package (VASP) code. Projector-augmented wave (PAW) approach was used to describe the ion-electron interactions.[2] According to our test results, we adopted the revised Perdew–Burke–Ernzerhof (RPBE) functional to describe the exchange-correlation interaction.[3] The cutoff energy for the plane-wave basis set was set to 500 eV. A larger than 15 Å vacuum layer was inserted along the z-axis direction to eliminate interactions between periodic images. K-point separation of at least 0.04 $Å^{-1}$ was employed. For the surface models, the bottom two atomic layers were fixed while other atoms were fully relaxed. The diffusion energy barrier on various Li surfaces was obtained by the climbing-image nudged elastic band (CI-NEB) method.[4]

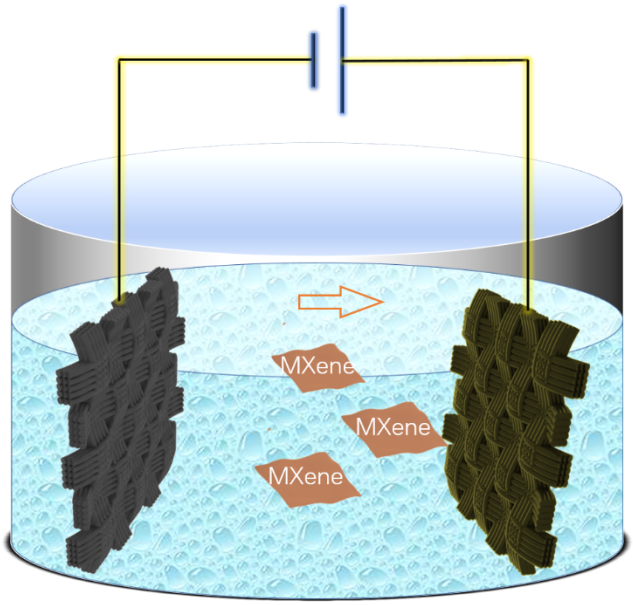

Fig. S1. Schematic diagram of electrophoretic deposition processes. MXene nanosheets will move toward the anode under a 5 V voltage difference because MXene is negatively charged.

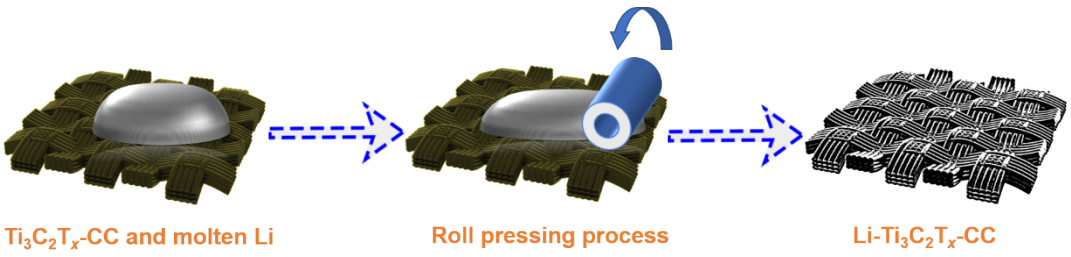

Fig. S2. Schematic diagram of Li-$Ti_3C_2T_x$-CC electrodes fabrication processes by a roll pressing procedure.

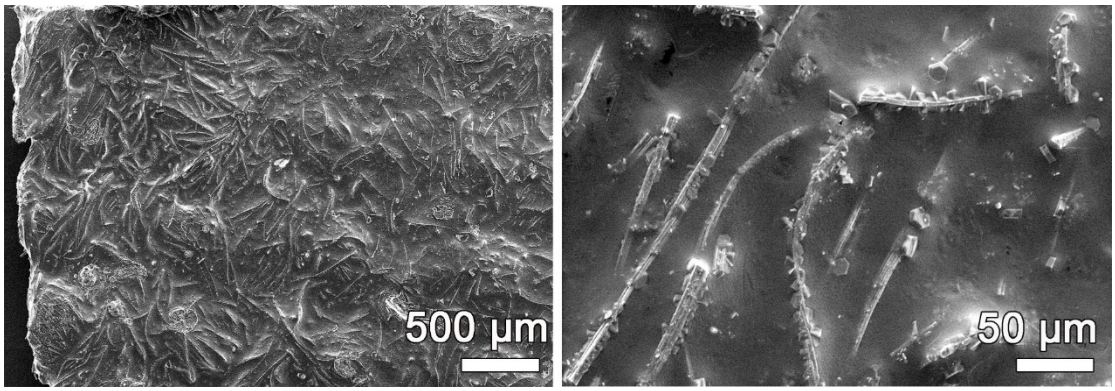

Fig. S3. SEM images of fully loaded Li-$Ti_3C_2T_x$-CC.

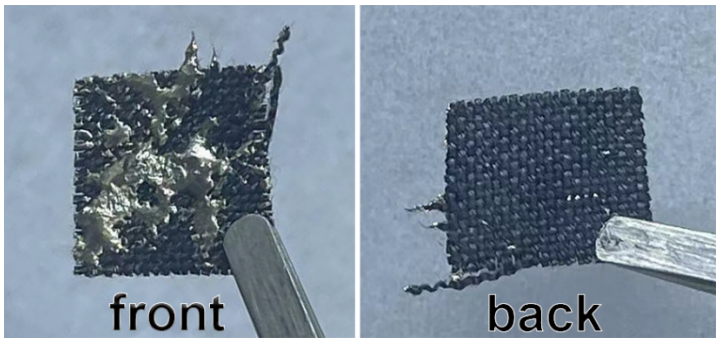

Fig. S4. Photos of Li-CC, with molten Li only sticking to the surface.

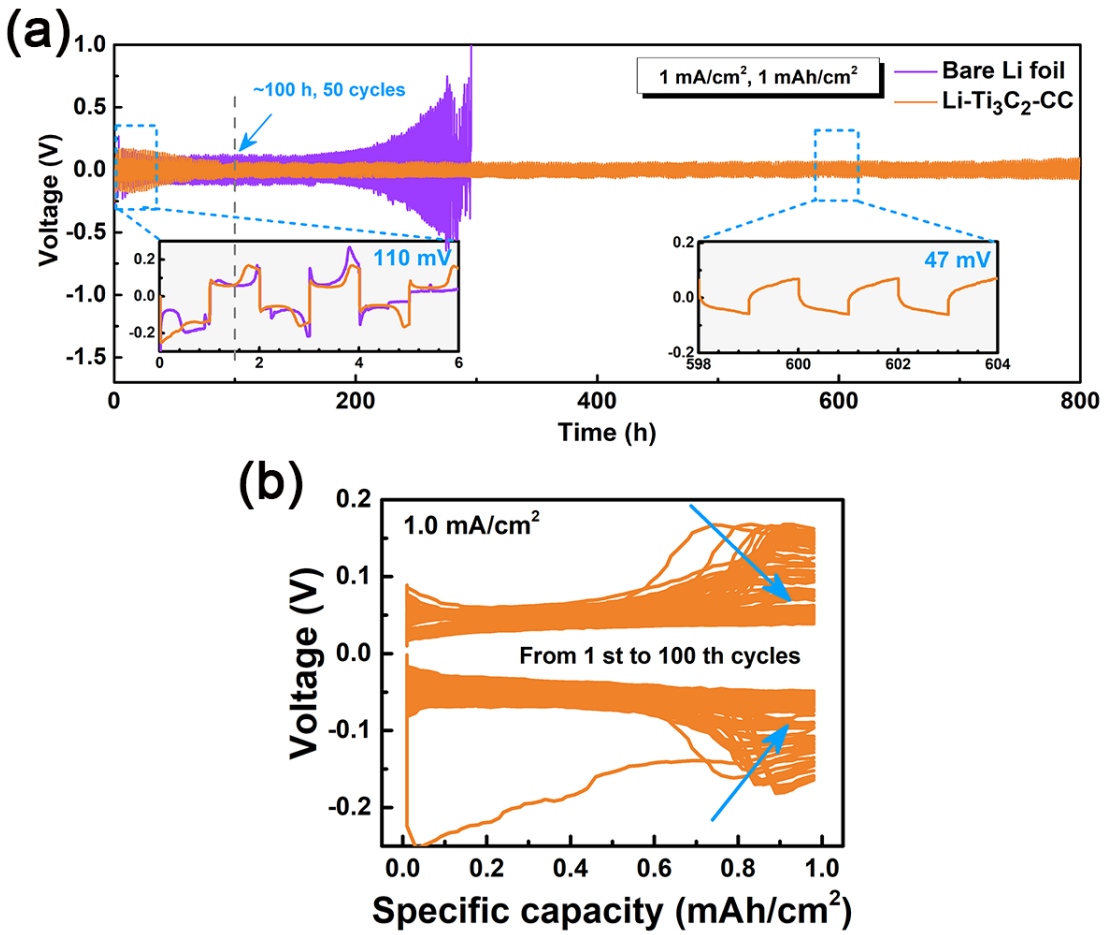

Fig. S5. (a) Cycling performance of bare Li and Li-$Ti_3C_2T_x$-CC at a current density of 1.0 mA·cm^{-2}. Initial voltage curves (illustration left), and voltage curves around 600 h (illustration right). **(b) Voltage-capacity curves of Li-$Ti_3C_2T_x$-CC at 1.0 mA·cm^{-2} for the initial 100 cycles, with a gradually smoothing process.**

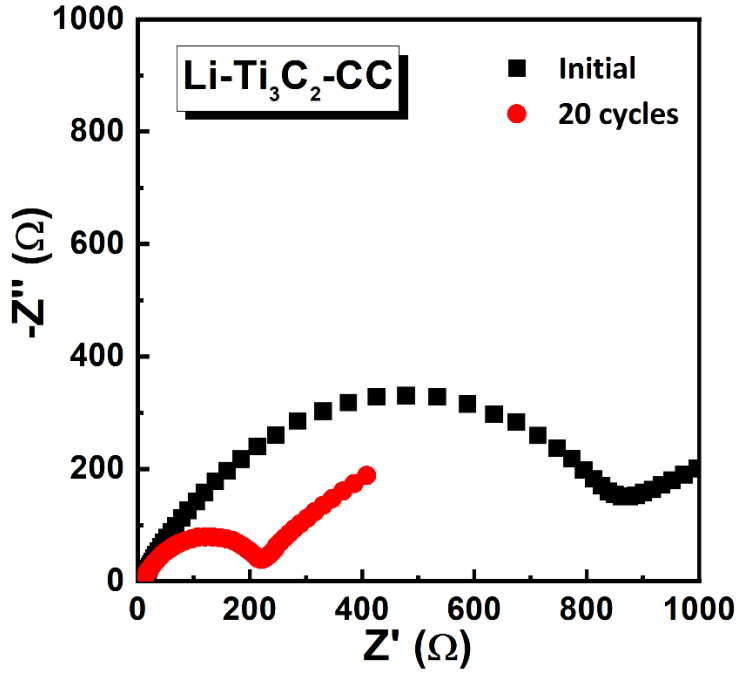

Fig. S6. Nyquist plots of Li-$Ti_3C_2T_x$-CC electrodes. Cycling current density was 1.0 mA·cm^{-2}.

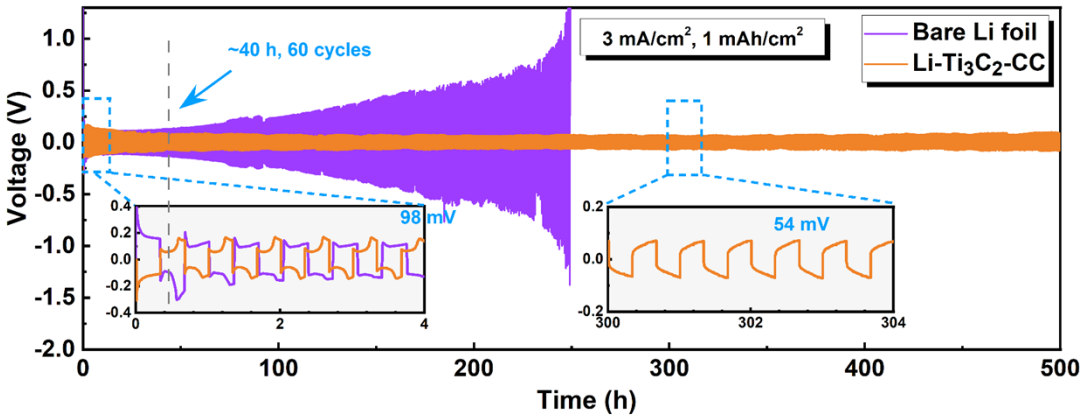

Fig. S7. Cycling performance of bare Li and Li-$Ti_3C_2T_x$-CC at a current density of 3.0 mA·cm^{-2}. Initial voltage curves (illustration left), and voltage curves around 300 h (illustration right).

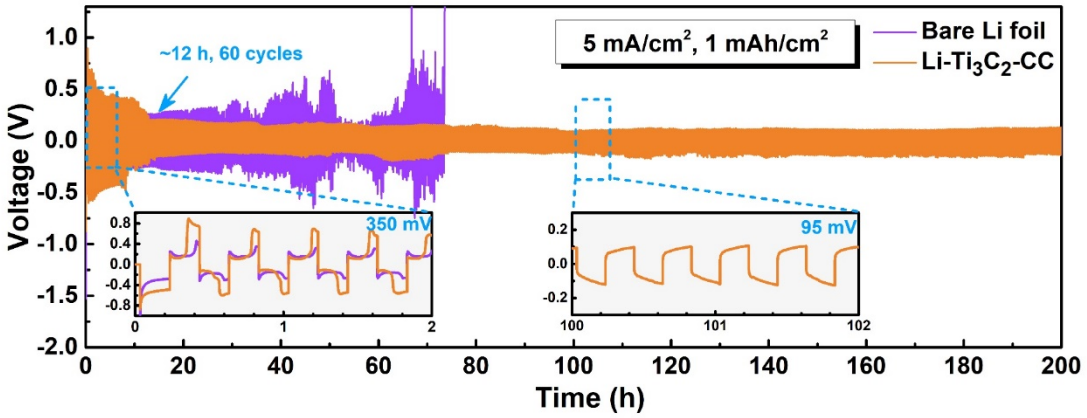

Fig. S8. Cycling performance of bare Li and Li-$Ti_3C_2T_x$-CC at a current density of 5.0 mA·cm^{-2}. Initial voltage curves (illustration left), and voltage curves around 100 h (illustration right).

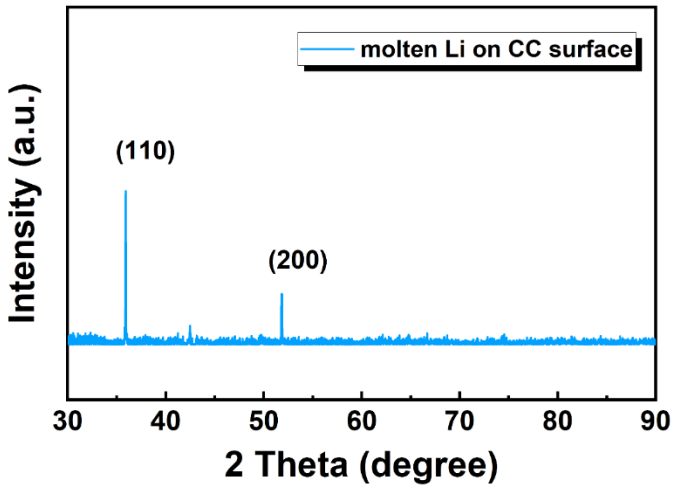

Fig. S9. XRD patterns of Li-CC.

The melting-cooling Li on the bare CC surface (Fig. S9) also shows more Li(110) facets (S_{110}/S_{200}=1.9) than bare Li (S_{110}/S_{200}=0.05), but less than Li-$Ti_3C_2T_x$-CC (S_{110}/S_{200}=2.7), indicating that both melting-cooling process and MXene play important roles of the initial formation of Li(110)..

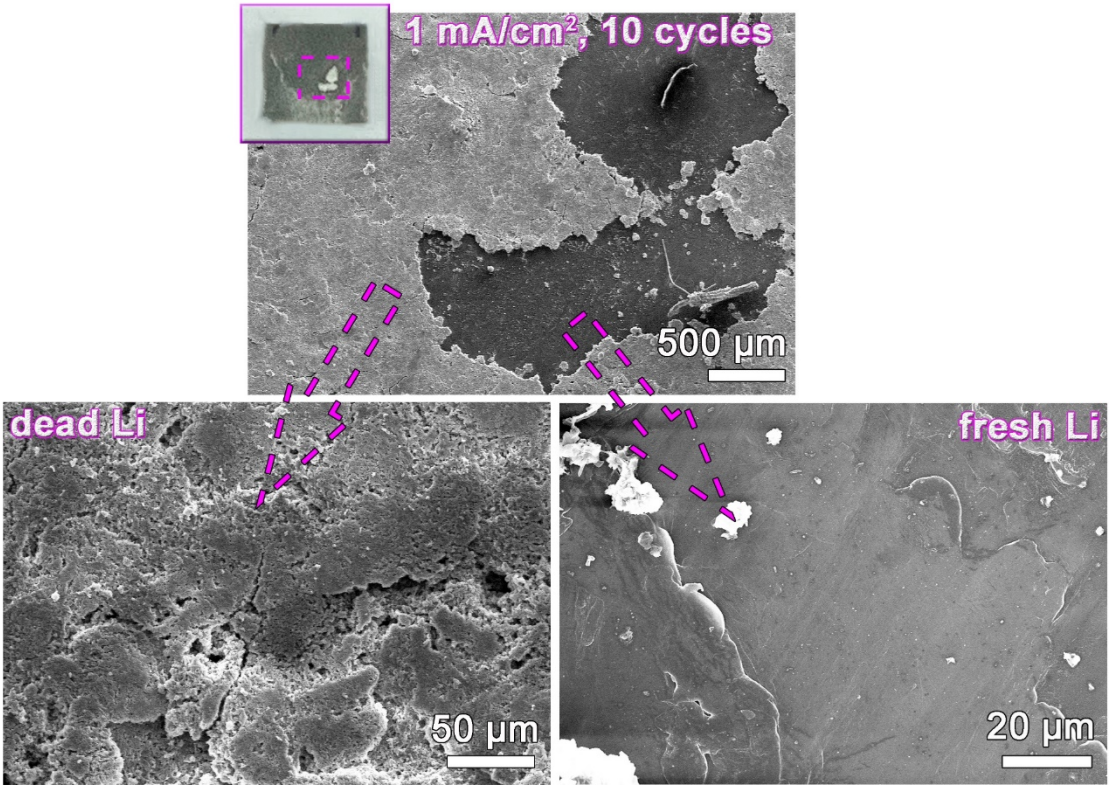

Fig. S10. SEM of bare Li electrodes after 10 cycles at a current density of 1.0 mA·cm^{-2}. The illustration at the top left corner is a digital photo of this electrode.

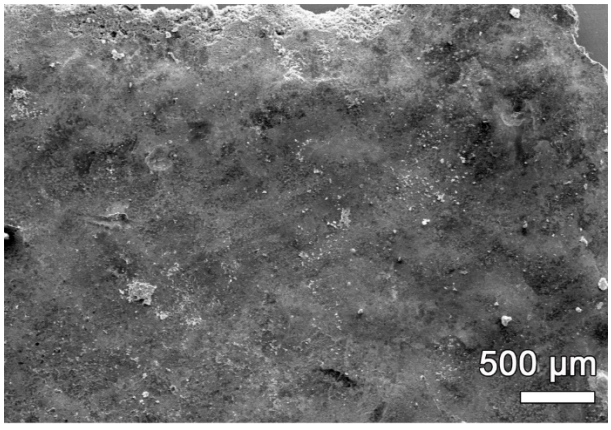

Fig. S11. SEM of Li-$Ti_3C_2T_x$-CC electrodes after 200 cycles (80 h) at a current density of 5.0 mA·cm^{-2}.

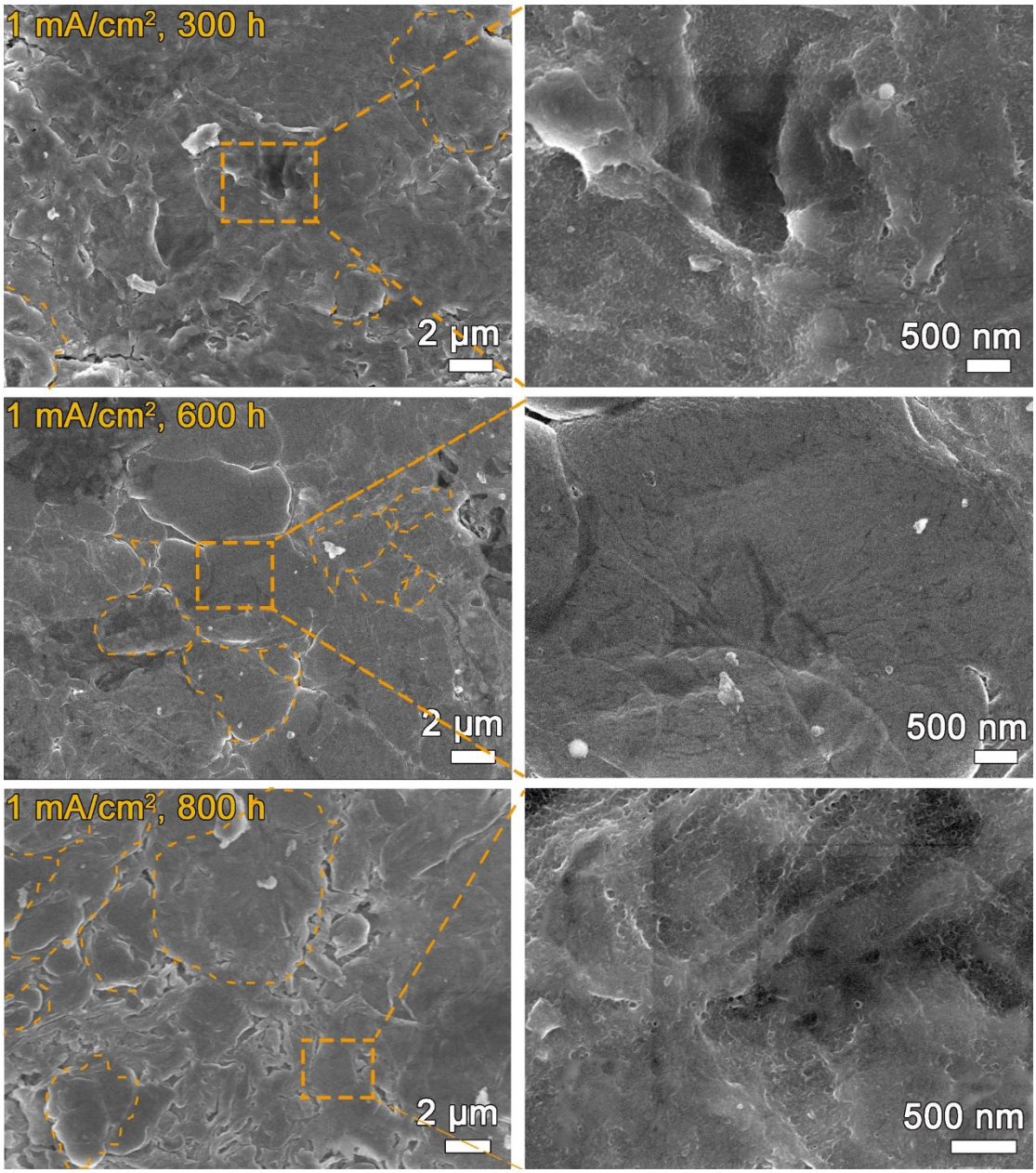

Fig. S12. Interface morphology evolution of Li-$Ti_3C_2T_x$-CC electrodes after 300, 600, and 800 h cycling at a current density of 1.0 mA·cm^{-2}.

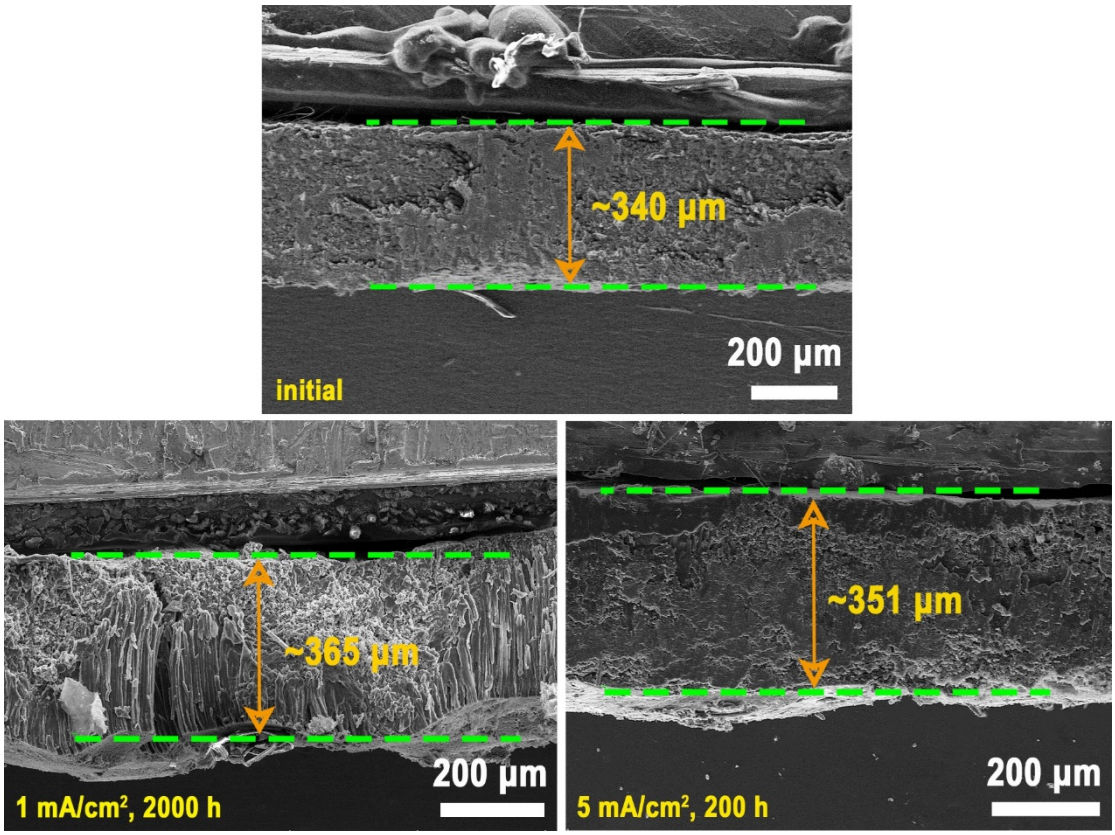

Fig. S13. Thickness changes of Li-$Ti_3C_2T_x$-CC after cycling.

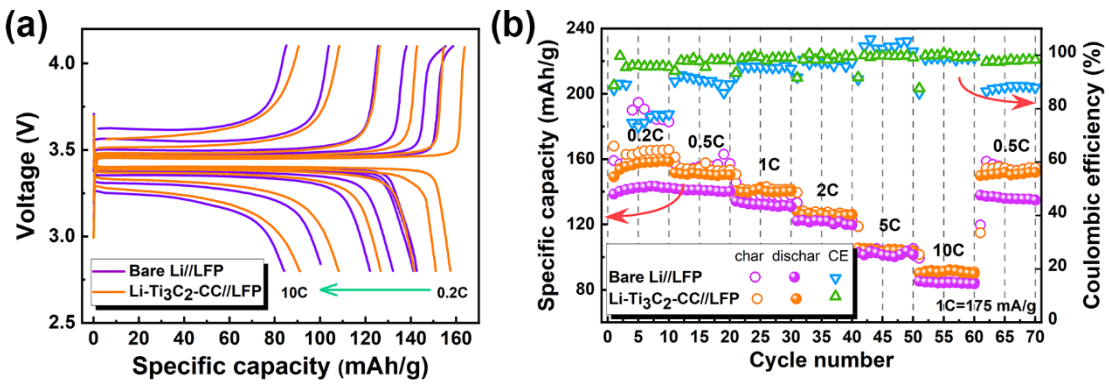

Fig. S14. Electrochemical performance batteries with $LiFePO_4$ (LFP) as the cathode and bare Li or Li-$Ti_3C_2T_x$-CC as the anode. (a) Charging-discharging curves and (b) rate performance from 0.2 C to 10 C (1 C=175 $mA \cdot g^{-1}$).

The batteries with Li-$Ti_3C_2T_x$-CC anodes show larger average specific capacity, smaller polarization and higher Coulomb efficiency than those with bare Li anodes.

References

1. P. Collini, S. Kota, A. D. Dillon, M. W. Barsoum and A. T. Fafarman, *J. Electrochem. Soc.,* 2017, **164**, D573-D580.
2. G. Kresse and D. Joubert, *Phys. Rev. B,* 1999, **59**, 1758-1775.
3. B. Hammer, L. B. Hansen and J. K. Nørskov, *Phys. Rev. B,* 1999, **59**, 7413-7421.
4. G. Henkelman and H. Jónsson, *J. Chem. Phys.,* 2000, **113**, 9978-9985.